Multi-Scale Individual-Based Model of Microbial and Bioconversion Dynamics in Aerobic Granular Sludge

JOAO B. XAVIER,*,†
MERLE K. DE KREUK,‡
CRISTIAN PICIOREANU,‡ AND
MARK C. M. VAN LOOSDRECHT‡

Biomathematics group, Instituto de Tecnologia Química e Biológica, Universidade Nova de Lisboa, R. Qta Grande 6, 2780 Oeiras, Portugal, Department of Biotechnology, Delft University of Technology. Julianalaan 67, 2628 BC Delft, The Netherlands

Aerobic granular sludge is a novel compact biological wastewater treatment technology for integrated removal of COD (chemical oxygen demand), nitrogen, and phosphate charges. We present here a multiscale model of aerobic granular sludge sequencing batch reactors (GSBR) describing the complex dynamics of populations and nutrient removal. The macro scale describes bulk concentrations and effluent composition in six solutes (oxygen, acetate, ammonium, nitrite, nitrate, and phosphate). A finer scale, the scale of one granule (1.1 mm of diameter), describes the two-dimensional spatial arrangement of four bacterial groups—heterotrophs, ammonium oxidizers, nitrite oxidizers, and phosphate accumulating organisms (PAO)—using individual based modeling (IbM) with species-specific kinetic models. The model for PAO includes three internal storage compounds: polyhydroxyalkanoates (PHA), poly phosphate, and glycogen. Simulations of long-term reactor operation show how the microbial population and activity depends on the operating conditions. Short-term dynamics of solute bulk concentrations are also generated with results comparable to experimental data from lab scale reactors. Our results suggest that N-removal in GSBR occurs mostly via alternating nitrification/denitrification rather than simultaneous nitrification/denitrification, supporting an alternative strategy to improve N-removal in this promising wastewater treatment process.

Introduction

Aerobic granular sludge sequencing batch reactors (*1*–*7*) are an attractive alternative to conventional activated sludge processes for wastewater treatment thanks to a compact design (*8*) with a footprint of only 25% relatively to conventional activated sludge systems. This compact design is possible partially due to the high settling velocity of the granular sludge that renders the use of the traditional settler—indispensable in the classical activated sludge process—

unnecessary. This process also allows high substrate loading rates (*9*) thanks to the high biomass concentrations achieved.

The compact design of granule sequencing batch reactors (GSBR) is also due to its integrated N-removal capabilities, possibly occurring through simultaneous nitrification/denitrification (SND). For SND to occur in aerobic granules, both an aerobic zone for nitrification and an anoxic substrate-rich interior for denitrification must exist within the same granule. The coexistence of an outer aerobic shell and an inner anaerobic zone is largely dependent on the bulk concentration of oxygen. However, whereas nitrification is favored by a high oxygen concentration, lower oxygen concentrations increase the size of the inner anaerobic zone where denitrification may occur. A previous one-dimensional modeling study (*10*) has determined that a DO value of 40% (3.2 mgO$_2$/L) would be optimal for SND.

GSRB operation was recently improved by introducing an anaerobic feeding phase. This provided selective pressure for slower growing organisms resulting in improved granular sludge stability (*11*). With this, the anaerobic/aerobic cycle provided conditions for the proliferation of polyphosphate-accumulating organisms (PAO) if enough phosphate was provided and the sludge residence time is suitably controlled. PAO are capable of storing poly phosphate (poly-P) as an energy reserve, a process in which polyhydroxyalkanoates (PHA) and glycogen are also involved (*12*), generating biological phosphate removal.

Integrated removal of chemical oxygen demand (COD), nitrogen and phosphate is achieved by a combination of several bioconversion carried out by multiple microbial groups coexisting in aerobic granules (*13*). Understanding how the operating conditions influence the composition of this microbial population and, consequently, the reactor performance is key for process engineering. For this purpose, we introduce a multiscale model the GSBR that uses individual based modeling (IbM) of the microbial population in the granule integrated here for the first time with reactor-scale sequencing batch dynamics. IbM was introduced to microbial populations by Kreft et al. (*14*) and, while being particularly suited to address ecological and evolutionary questions (*15, 16*), was applied previously to several environmental bioprocesses involving biofilms and filamentous sludge (reviewed in ref*17*) and anaerobic granules (*18*). IbM was recently made more accessible by a framework for multispecies biofilm modeling (*19*) which also facilitates the customized description of diverse microbial species metabolism with structured biomass. This framework was extended here to describe aerobic granular sludge process.

Materials and Methods

Model Description. We consider here three spatial scales (Figure 1). The *individual scale* describes the metabolism of individual biomass elements. The *granule scale* describes the spatial structure of the aerobic granule. The *reactor scale* describes dynamics of the entire reactor (i.e., bulk concentration of all solutes and total amount of biomass). The system modeled here is a lab scale GSBR (3 L volume) used previously in several experimental studies (*13*).

The kinetic model for the bioconversions is based on the activated sludge model no. 1 (ASM1) with the addition of metabolic description of PAO and separate description of ammonium and nitrite oxidizing bacteria (*20*). The kinetic model is composed by the 18 bioreactions (described in tables T1–T4 of the Supporting Information). Figure 2 represents the metabolism of the four microbial groups.

* Corresponding author phone: +1 617 384 9920; fax: +1 617 495 2196; e-mail: jxavier@cgr.harvard.edu.
† Universidade Nova de Lisboa. Present address Harvard University.
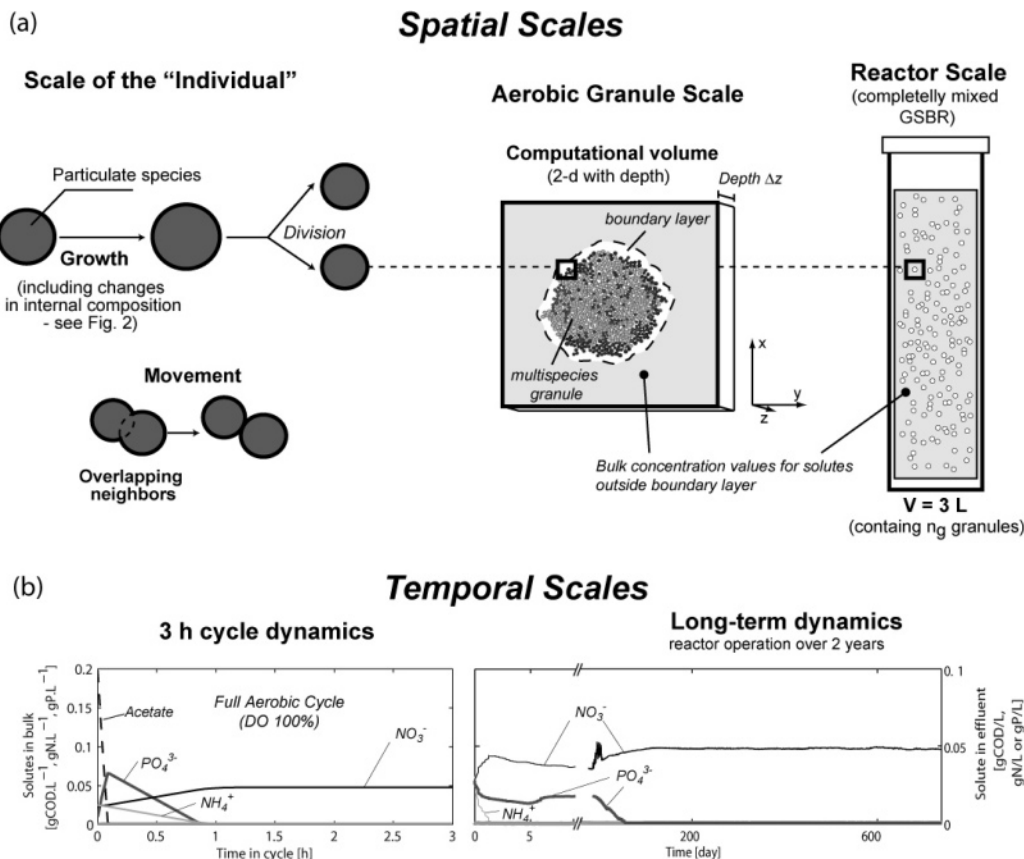‡ Delft University of Technology.

FIGURE 1. The spatial and temporal scales of the multi-scale model. (a) Spatial scales range from individual biomass elements, at a scale of a few micrometers to dynamics of multiple bacterial groups in the "aerobic granule scale", in millimeter scale, to the full system (a 3 L lab scale GSBR). The 2-D computational domain represents a small subvolume inside the reactor containing a single granule. The number of granules in the reactor (n_g) is a multiplier used for scaling-up the granule scale mass balances to the bulk concentrations dynamics (eq 1). The computational domain is given a depth, Δz, for mass balancing purposes, as previously described for 2-D biofilm simulations (19). (b) Temporal scales range from "short-term dynamics" describing each 3-h cycle with precision, to "long-term dynamics" in which GSBR operation is simulated over 2 years.

TABLE 1. Aeration Regimes for the Six Simulations[a]

simulation no.	aeration regime	DO during aeration	representing experimental conditions from the following::
1	continuous aeration	100%	25
2		40%	21
3	anaerobic phase (1h) followed by continuous aeration (2 h)	40%	11
4		20%	13
5	anaerobic phase (1h) followed by on/off controlled aeration (2 h)	40%	not tested experimentally

[a]Dissolved oxygen (DO) represents the percentage from the saturation concentration, here considered to be 8 mg_{O2}/L.

We consider six solute species: oxygen (S_{O2}), acetate (substrate, S_{Ac}), ammonium (S_{NH4}), nitrite (S_{NO2}), nitrate (S_{NO3}), and phosphate (S_{PO4}). A seventh species, dinitrogen gas (S_{N2}) is produced by denitrification reactions and considered for mass balances purposes. N_2 does not influence any of the reaction kinetics because it is an inert end-product of ammonia oxidation released to the atmosphere. We consider eight particulate species: active mass of ammonium oxidizing bacteria (X_{NH}), active mass of nitrite oxidizing bacteria (X_{NO}), active mass of heterotrophic bacteria (X_H), active mass of phosphate accumulating organisms (X_{PAO}), the internal storage polymers PHA (polyhydroxyalcanoates, X_{PHA}), poly phosphate (poly-P, X_{PP}) and glycogen

(X_{GLY}), and inerts (X_I). Individual biomass elements belong to one of the following four bacteria groups: ammonia oxidizing bacteria (NH), nitrite oxidizing bacteria (NO), nonphosphate accumulating heterotrophs (H), and phosphate accumulating organisms (PAO). The active species present in one individual defines its bacterial group. In addition, individuals of all four species may have a fraction of inerts resulting from the decay.

The 3 L lab-scale reactor is operated in a 3 h cycle. At the end of each cycle the reactor is half-emptied, following typical operation (13). A volume of 1.5 L of fresh feed is then added to refill the reactor before a new cycle begins. Both the emptying and refilling operations are assumed to be instantaneous; i.e. substrate concentration becomes the volume weighted average from the substrate concentrations in influent and that remaining in the reactor. Dynamics of bulk concentrations of each solute during each 3 h cycle are described generally as

$$\frac{dS_{i,bulk}}{dt} = n_g R_i(t) \ [M_i L^{-3} T^{-1}] \qquad (1)$$

where n_g is the number of granules in the reactor, and R_i is the global conversion rate of the solute i in by a single granule. Conversions by nongranular biomass suspended in bulk liquid are here neglected (see below).

The dynamics of dissolved oxygen is not modeled by eq 1. Instead, three aeration scenarios are considered. The first assumes a constant DO during the entire 3 h cycle, such as

that carried out in earlier lab-scale studies (*10, 21*). The second regime consists of aerobic/anaerobic phases during the cycle. Here, bulk concentration of oxygen is set to zero in the first hour, and to a value $S_{O2,aeration}$ during the following 2 h, as carried out in more recent studies (*11, 13*). The third regime is a variation of the later aeration strategy where the aerobic phase will be subject to on/off control dependent on the concentration of ammonia (*20*).

The computational domain represents a 2 d median cross-section of a single granule. Simulations start with 10 equally sized particles of each of the four microbial groups, constituting a granule of 120 μm. As in previous models (*19*), spatial solute distributions can be calculated from a steady-state diffusion−reaction equation for each of the solutes since diffusion is much faster than microbial growth:

$$D_i\left(\frac{\partial^2 S_i}{\partial x^2} + \frac{\partial^2 S_i}{\partial y^2}\right) + r_i = 0 \ [M_i L^{-3} T^{-1}] \qquad (2)$$

D_i is the diffusivity of species i and r_i is the local conversion rate of i. Equation 2 is solved in the granule and in the surrounding concentration boundary layer. Complete mixing of the bulk liquid is assumed for the rest of the computational domain ($S_i = S_{i,bulk}$).

Equations for the local bioconversion rates are depicted in Table T1 (Supporting Information). The local values of solute concentrations are used as bioconversions produce local changes in particulate species, thus altering the biomasses of individuals. To illustrate this concept, consider the case of poly-P. Poly-P is involved in four processes: storage of acetate ($r_{SA}^{(AN)}$), aerobic storage of poly-P ($r_{PP}^{(O2)}$), nitrate- and nitrite-using storage of poly-P ($r_{PP}^{(NO3)}$ and $r_{PP}^{(NO2)}$). The expression defining the net rate of poly-P, r_{PP}, in a PAO biomass element is

$$r_{PP} = \frac{dm_{PP}}{dt} = -Y_{PO_4}r_{SA}^{(AN)} + r_{PP}^{(O2)} + r_{PP}^{(NO3)} +$$

$$r_{PP}^{(NO2)} = -Y_{PO_4}q_{s,max}\cdot\frac{S_{Ac}}{S_{Ac} + K_{AP}}\cdot$$

$$\frac{f_{PHA,max} - f_{PHA}}{(f_{PHA,max} - f_{PHA}) + K_{PHAP}}\cdot\frac{f_{PP}}{f_{PP} + 0.1}\cdot m_{PAO} +$$

$$k_{PP}\cdot\frac{S_{O_2}}{S_{O_2} + K_{O_2,P}}\cdot\frac{f_{PP,max} - f_{PP}}{(f_{PP,max} - f_{PP}) + K_{PP,P}}\cdot\frac{S_{PO_4}}{S_{PO_4} + K_{PO_4,P}}\cdot m_{PAO} +$$

$$k_{PP}\cdot\eta_{NO_2}\cdot\frac{S_{NO_2}}{S_{NO_2} + K_{NO_2,H}}\cdot\frac{K_{O_2,PAO}}{S_{O_2} + K_{O_2,H}}\cdot$$

$$\frac{f_{PP,max} - f_{PP}}{(f_{PP,max} - f_{PP}) + K_{PP,P}}\cdot\frac{S_{PO_4}}{S_{PO_4} + K_{PO_4,P}}\cdot m_{PAO} +$$

$$k_{PP}\cdot\eta_{NO_3}\cdot\frac{S_{NO_3}}{S_{NO_3} + K_{NO_3,H}}\cdot\frac{K_{O_2,PAO}}{S_{O_2} + K_{O_2,H}}\cdot$$

$$\frac{f_{PP,max} - f_{PP}}{(f_{PP,max} - f_{PP}) + K_{PP,P}}\cdot\frac{S_{PO_4}}{S_{PO_4} + K_{PO_4,P}}\cdot m_{PAO}$$

$$[M_{PP}T^{-1}\cdot particle^{-1}] \quad (3)$$

Notations used here are defined in tables T1−T5 (Supporting Information). Production and consumption of poly-P in the biomass particles are accompanied by its uptake and release respectively. The phosphate rate is

$$r_{PO_4} = \frac{dS_{PO_4}}{dt} = Y_{PO_4}r_{SA}^{(AN)} - r_{PP}^{(O2)} - r_{PP}^{(NO3)} -$$

$$r_{PP}^{(NO2)} \ [M_{PO_4}T^{-1}\cdot L^{-3}] \quad (4)$$

Because r_{PO_4} reflects the change in phosphate concentration

at the location of the biomass particle, the biomass m_{PAO} in eq 3 is replaced by the biomass concentration X_{PAO} when computing rates in eq 4. Rate r_{PO_4} is the partial contribution of a single biomass particle to the net bioconversion rate of phosphate of the entire granule, $r_{PO_4,g}$. The rate per granule comes from the contributions of all biomass particles composing it at a given instant:

$$r_{PO_4,g} = \sum_{\substack{particles \\ in\ the\ granule}} r_{PO_4} \ [M_{PO_4}T^{-1}.granule^{-1}] \qquad (5)$$

The net rate per granule is multiplied by the number of granules in the reactor to produce the conversion rate at the reactor-scale, $r_{PO_4,bulk}$:

$$r_{PO_4,bulk} = \frac{dS_{PO_4,bulk}}{dt} = n_g r_{PO_4,g} \ [M_{PO_4}T^{-1}\cdot L^{-3}] \qquad (6)$$

The N- and P-content in active biomass are neglected. N- and P-content of biomass have typical values of 0.07 gN·gCOD^{-1} and 0.02 gP·gCOD^{-1} respectively (*22*). This simplification greatly speeds up computation time (twice faster) at the expense of slight underestimations of N- and P-removals.

A maximum granule diameter of 1100 μm is set here, a typical average granule size found in our lab-scale reactors. Biomass growing beyond this limit is removed by detachment. The effects of detached biomass on global bioconversions are neglected. This is a valid approximation since the small suspended biomass particles have a large settling time and, therefore, are rapidly removed from the reactor at the end of each 3 h cycle (see also Supporting Information Figure F4).

The long-term operation of the GSBR (730 days, 2 years) was simulated in five different cases considering different aeration regimes. The simulation of long periods is necessary to determine the stability of apparent steady states. Table 1 lists the aeration conditions used for the simulations carried out. The simulations required heavy computation and were carried out in dual-processor Intel(R) Xeon CPU 3.2 GHz computers taking about 8 days for each simulation. Animations produced from the simulations are available in the Supporting Information.

Results

Figure 1b shows the short term and long-term dynamics of the bulk concentrations of solutes in one cycle and in the effluent respectively. More detailed results for the time courses of the granule composition and effluent concentrations for the five simulations may be found in Figure F1 of the Supporting Information. Figure F2 (Supporting Information) shows results from typical 3 h cycles from the mature stages of GSBR operation. *Mature stage* is here defined as the period when both granule composition and effluent concentrations become stationary. Next, we comment on the results from case no. 1. Finally, the remaining simulation results are briefly described, referring to the differences from case no. 1.

Initial Development Stage. This case describes a continuously aerated system at a high dissolved oxygen concentration, mimicking the conditions of experiments reported in ref *4*. Initial development stage is the period in which the granule grows up to the maximum diameter of 1100 μm, which then lasts 30 days. During this period, the non-PAO heterotrophic population (H) grow very rapidly quickly becoming the dominant bacterial group in the granule (see Figure 3a−f). Complete acetate removal is achieved in the second cycle, dividing the cycle into a period when acetate is present, called *feast phase*, and *famine phase* (*10*). The
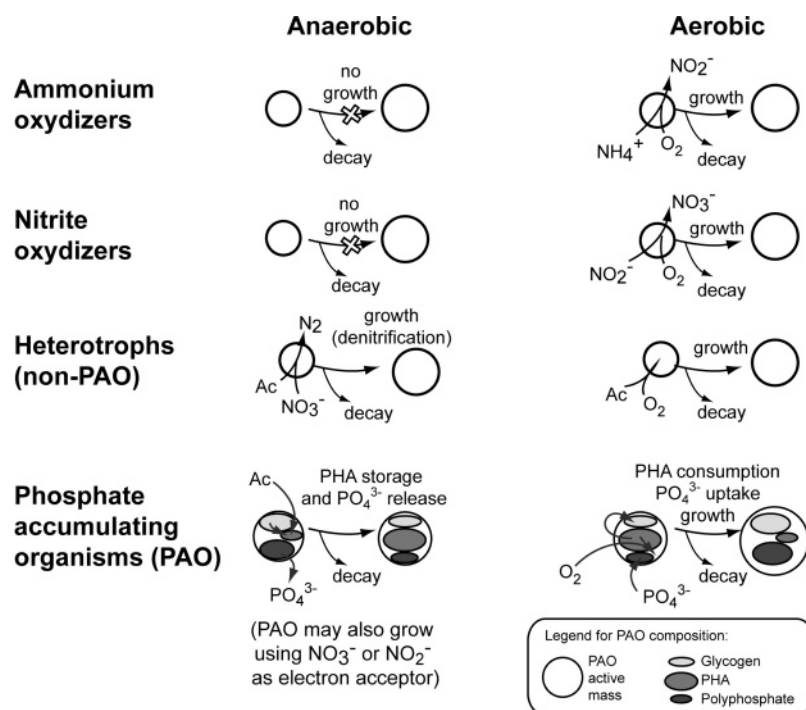
FIGURE 2. Schematic representation of the bioreactions carried out in individuals of the four microbial groups. Bioreactions are detailed in tables T1 and T2 (Supporting Information). Not represented here, but implemented in the model, is the capability of PAO carrying out PHA consumption, phosphate ("PO_4^{3-}") uptake and growth using nitrite ("NO_2^-") and/or nitrate ("NO_3^-") in the absence of O_2. "Ac" represents acetate.
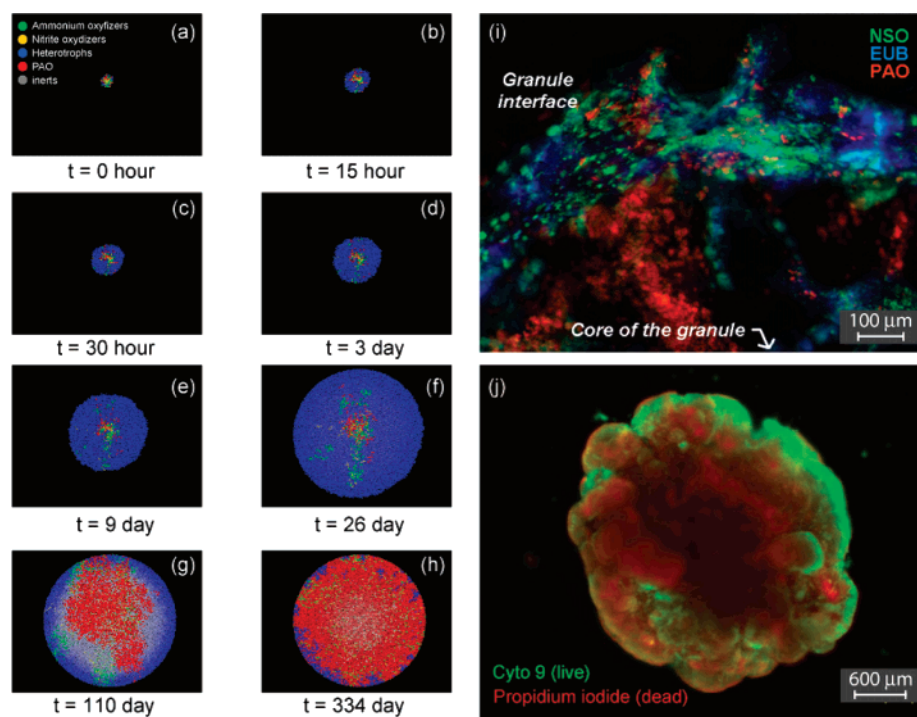

FIGURE 3. Spatial distributions of microbial populations and inert materials in aerobic granules. (a−h) Granule development for simulated case no. 1. Initially, fast growing heterotrophic organisms (in blue) constitute the majority of the granule biomass at day 26. In later stages, phosphate accumulating organisms (in red) dominate in spite of growing at a slower rate, since they make a more efficient use of the substrate consumed. (i) Fluorescence in-situ hybridization (FISH) of microbial groups in the granule visualized using confocal laser scanning microscopy (green is ammonium oxidizing bacteria; blue is eubacteria; red is PAO, reproduced with authorization from ref 13); (j) Mature granule from lab scale GSBR stained with live/dead kit (Molecular Probes, Eugene, OR), showing accumulation of inert material, stained red by propidium iodide, in the granule core, whereas live bacteria, stained green with Cyto-9, are located in the outer layers, similarly to what was obtained from simulations (i.e., panels g and h).

feast phase is characterized by strong oxygen gradients throughout the granule, with the outer layers having a high oxygen concentration and the core of the granule experienc- ing anaerobic conditions. Gradients are caused by the high rate of oxygen consumption by heterotrophic bacteria consuming acetate aerobically. In contrast, in the famine
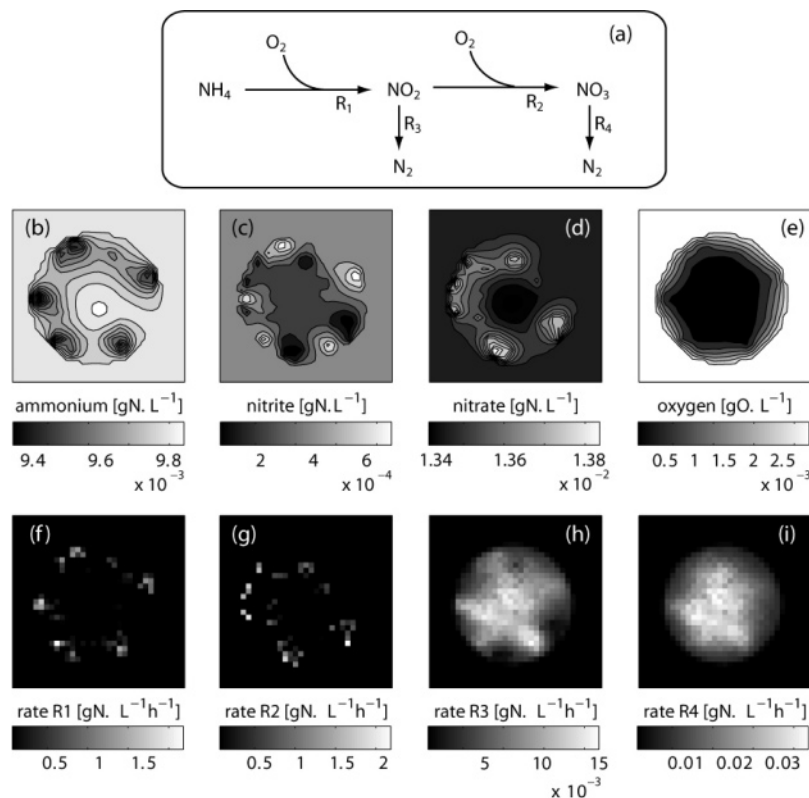
FIGURE 4. Detailed insight into the spatial localization of bioconversions is provided by 2-D simulations. Here, a snapshot of the N-conversions at 1.75 h into a cycle at day 600 for simulation no. 3. (a) The nitrification/denitrification pathway. Two-dimensional distributions of ammonium (b), nitrite (c), nitrate (d), and oxygen (e) concentrations; 2-D localization of N-bioconversions discriminated as ammonium oxidation (nitrification, pane f), nitrite oxidation (g), denitrification on nitrite (h), and denitrification using nitrate (i) are also shown. See tables T1 and T2 in the Supporting Information for the expression rates used for R1−R4.

phase oxygen penetrates well into the granule. Growth of ammonia oxidizers is only possible in famine phase when competition for oxygen is lower. Growth of ammonium oxidizers is low in the initial period but sufficient for complete NH_4^+ removal to be achieved by day 3. Any NO_2^- produced by ammonium oxidizers is rapidly converted to NO_3^- by nitrite oxidizers. Growth of PAO is low and phosphate removal at day 30 is only 10%. By day 30, inerts already constitute more than 50% of the granule mass, originated mostly from the decay of heterotrophs.

Maturation. After reaching maximum granule size, the maturation phase begins with the internal composition of the granule rearranging itself until it stabilizes at day 150. During this period, heterotrophs start losing their dominance in favor of PAO, which steadily grow from the inside of the granule (see sequence of Figure 3f−h). Enrichment in PAO increases phosphate removal, with cyclic phosphate release/uptake resulting in full phosphate removal at day 90. Ammonium oxidizers remain stable, sustaining complete NH_4^+ conversion.

The Mature Stage. It is only when PAO biomass is removed from the reactor through the process of detachment that actual phosphate removal from the system begins. Before this, phosphate is simply stored inside the granules in the form of poly-P (23). The mature stage that is characterized by a stable microbial population. The concentrations of storage compounds in PAO (PHA, poly-P, and glycogen) oscillate in each cycle (Supporting Information Figure F2c), with feast-phase accumulation of PHA and poly-P and glycogen consumption followed by famine-phase accumulation of poly-P and glycogen with PHA consumption. The average radial distribution of microbial groups (Supporting Information Figure F2d) is in general agreement with the

well-known layering observed in biofilms in the presence of different electron acceptors and the organization observed from imaging of FISH stained granules (Figure 3i). The organisms consuming substrate at the lowest redox state grow in the depth of the biofilm. Within each redox zone, the faster growing bacteria will be found more at the outside of the biofilm, where substrates are coming from. At the end of simulations, the major component of the granule is inert material (Figure 5a). Inerts are mostly located in the core, in agreement with microcopy imaging of Live/dead stained granules (Figure 3j) and a previous study by McSwain et al. where proteins, extracellular polymers and bacteria cells where stained simultaneously (24). The latter also showed also that this inert core is mostly composed by proteins.

Lower Operation DO, Case No. 2. As in case no. 1, initial development is characterized by predominance of heterotrophs, albeit less pronounced since lower DO is advantageous to PAO due to an increased anaerobic region. Consequently, complete P-removal can be achieved sooner (Figure F1d, Supporting Information). Inert accumulation is also faster, and the mature stage reached earlier at day 110. Composition in ammonia and nitrite oxidizers is practically not altered by the lower DO, but N-removal increases to 11%.

Anaerobic/Aerobic Cycle at DO 40%, Case No. 3. The competitive advantage of PAO is enhanced as soon as the feast phase becomes completely anaerobic. This anticipates slightly the full P-removal (Figure F1f, Supporting Information). However, since ammonium oxidation is only possible in the aeration period, N-conversions take longer to stabilize. The mature stage is characterized by a larger fraction of PAO in the granule (Figure 5b). Phosphate and acetate conversions
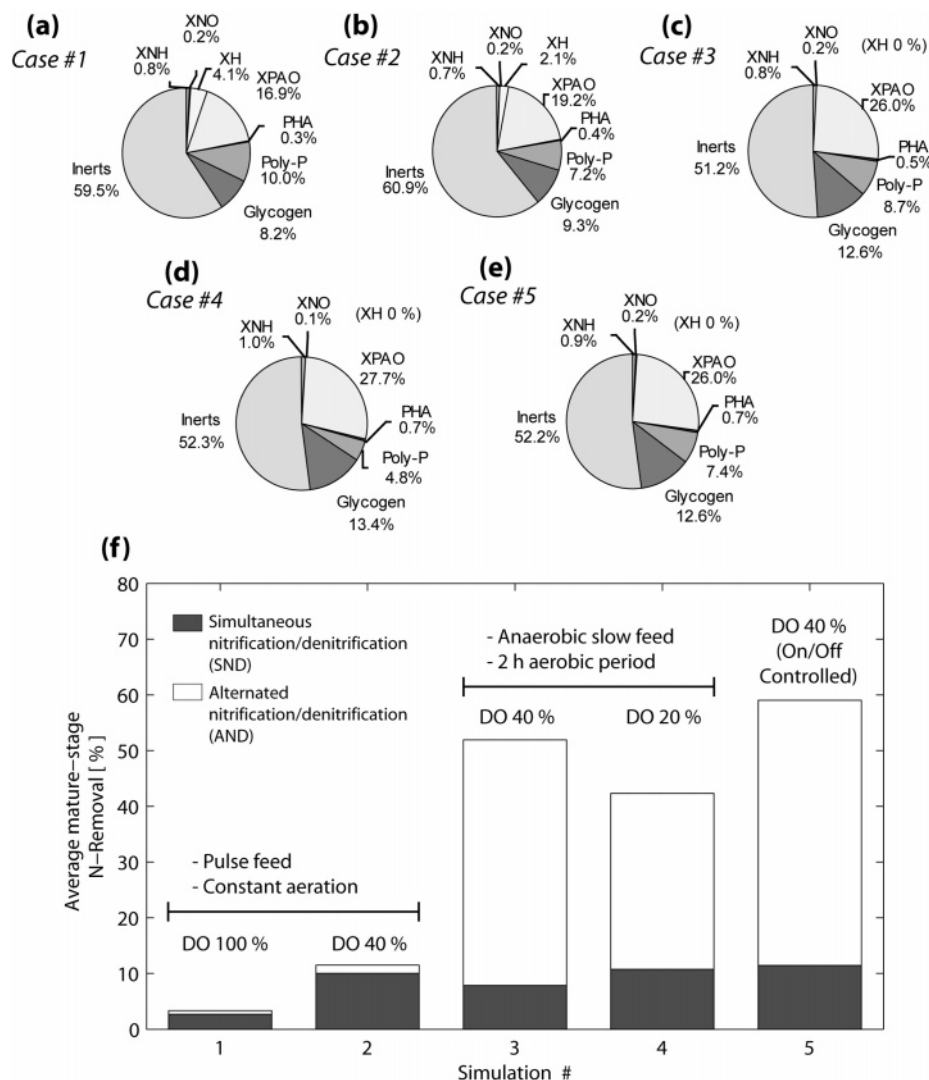
FIGURE 5. Mature stage characteristics of granule and the N-removal efficiency for different operating conditions. (a—e) Granule composition in the mature stage for all simulations. (f) The N-removal is the result of simultaneous nitrification/denitrification (SND, dark areas in bars) and that resulting by alternated nitrification/denitrification (AND, white areas in bars). These results show that attempts to increase N-removal by operating the reactor at lower DO, supposedly to increase SND, are only marginally successful. Instead, N-removal is significantly enhanced when operational changes create improved conditions for AND, such as in case nos. 3, 4, and 5, which have anaerobic periods in the operation cycle.

are still complete and N-removal increases significantly to 50%.

Anaerobic/Aerobic Cycle at DO 20%, Case No. 4. This simulation predicts that very low DO has a negative effect on all bioconversions. Full P-removal is significantly delayed and complete conversion of ammonia to nitrate may never fully achieved (Figure F1h, Supporting Information). Effluent concentrations of N-components oscillate constantly and the net N-removal is 40%.

Introducing On/Off Control of DO, Case No. 5. Operating conditions of this simulation are identical to those of case no. 3, with the additional control of aeration. Aeration is switched off during the aerobic phase once ammonia is completely consumed. This results in an increase of N-removal to 60%, the highest of all cases, in spite of only marginal changes in the composition of the microbial population (Figure 5e).

Further Comparison with Experimental Data. The simulated reactor-scale bioconversion dynamics were compared with the trends observed experimentally for solute species in the 3 h cycles. For the continuous aeration (case no. 1), the model results concerning acetate,

NH_4^+ and NO_3^- show qualitative agreement with trends measured by Beun et al. (25) who operated lab scale reactors in the same conditions. Comparisons with experimental results for the cases using anaerobic feeding phases are more difficult due to the impracticality of measuring concentrations during reactor feeding. Nevertheless, results for the aerated phase agree well (Figure F3, Supporting Information).

Discussion

Our simulations provide detailed insight into dynamics of the GSBR process. The present work focused on the effect of different aeration schemes. Nevertheless, the same model may be used to analyze other operating conditions that influence the microbial community such as the cycle duration (26), the influent composition (9), or the mechanical shear stress affecting granule size (27–31).

Attempts to improve N-removal in lab scale reactors have so far consisted in decreasing the operational DO of aerated phases in the GSBR cycle. These strategies are based on the assumption that nitrification and denitrification occur

simultaneously (13), in which case N-removal is enhanced by decreasing the oxygen penetration in the granule. Results from these simulations describe that simultaneous nitrification/denitrification (SND) is present to some extent (Figure 4). However, they also suggest that SND contribution to high nitrogen removal is limited. Figure 5f shows the relative contribution of SND to the total N-removal in all simulations. In the continuous aeration cases (nos. 1 and 2), total N-removal is low but SND accounts for the largest part. When anaerobic periods are introduced, as in cases 3 and 4, the overall N-removal becomes significantly higher. However, denitrification now occurs mainly during the anaerobic period, when nitrification is absent. In these cases, the nitrate being consumed at the beginning of the 3 h cycle is reminiscent from the previous cycle (see, for example, the black line representing S_{NO_3} in Figure F2i in the Supporting Information). This means that denitrification and nitrification occur in alternation. Realizing that most N-removal is due to alternating nitrification/denitrification (AND) rather than SND allows designing alternative strategies to further increase N-removal. This is the case of hypothetical on/off strategy proposed in case no. 5, that makes a second anaerobic phase later in the cycle (20). In reality, aeration cannot simply be switched off since it also provides mixing. Recycled off-gas (or N_2 in lab systems), could be sparged into the reactor to provide mixing but further experiments should evaluate the feasibility of a nonmixed system in the last cycle part.

This study demonstrates application of individual-based modeling (IbM) to the wastewater treatment process of aerobic granular sludge. These simulations provide insight into the many bioconversion processes occurring while describing both short-term dynamics and long-term reactor operation. This novel model integrates for the first time dynamics of microbial metabolisms, granule-scale diffusion-reaction with 2-D spatial organization and larger scale sequencing batch reactor operation. By being computationally demanding, these models are still far from having a disseminated application in process control. Nevertheless, they can already constitute a valuable research tool in academic and industrial research settings to study spatial-temporal dynamics in long-term development of multispecies microbial communities. The use of 2-D and 3-D models can often produce unexpected theoretical results that could not be predicted from 1-D models (16, 18, 32). Nevertheless, simpler 1-D biofilm models, such as the one in the popular AQUASIM software (33) that presently runs effortlessly in off-the-shelf desktop computers, have demonstrated the power of simulation for bioprocess design in environmental technologies. With the foreseeable increase in affordable computing power and efficient numerical methods, we may envision that multiscale individual-based models will be a common tool for the future engineer of biological wastewater treatment processes.

Nomenclature

AND	alternating nitrification/denitrification
COD	chemical oxygen demand
DO	dissolved oxygen (oxygen concentration as a percentage of its saturation in water)
GSBR	granular sludge sequencing batch reactor
IbM	individual-based modeling
PAO	phosphate accumulating organism
PHA	polyhydroxyalkanoates
poly-P	poly phosphate
S_i	concentration of solute species I
SND	simultaneous nitrification/denitrification
X_i	concentration of particulate species i

Supporting Information Available

Additional details are illustrated with five movies, five tables, and four figures. This material is available free of charge via the Internet at http://pubs.acs.org.

Literature Cited

(1) Tay, J. H.; Liu, Q. S.; Liu, Y. Aerobic granulation in sequential sludge blanket reactor. *Water Sci. Technol.* **2002**, *46* (4−5), 13−8.

(2) Etterer, T.; Wilderer, P. A. Generation and properties of aerobic granular sludge. *Water Sci. Technol.* **2001**, *43* (3), 19−26.

(3) Beun, J. J.; van Loosdrecht, M. C. M.; Heijnen, J. J., Aerobic granulation. *Water Sci. Technol.* **2000**, *41* (4−5), 41−48.

(4) Beun, J. J.; Hendriks, A.; van Loosdrecht, M. C. M.; Morgenroth, E.; Wilderer, P. A.; Heijnen, J. J., Aerobic granulation in a sequencing batch reactor. *Water Res.* **1999**, *33* (10), 2283−2290.

(5) Schwarzenbeck, N.; Borges, J. M.; Wilderer, P. A. Treatment of dairy effluents in an aerobic granular sludge sequencing batch reactor. *Appl. Microbiol. Biotechnol.* **2005**, *66* (6), 711−718.

(6) Schwarzenbeck, N.; Erley, R.; Mc Swain, B. S.; Wilderer, P. A.; Irvine, R. L. Treatment of malting wastewater in a granular sludge sequencing batch reactor (SBR). *Acta Hydrochim. Hydrobiol.* **2004**, *32* (1), 16−24.

(7) Schwarzenbeck, N.; Erley, R.; Wilderer, P. A. Aerobic granular sludge in an SBR-system treating wastewater rich in particulate matter. *Water Sci. Technol.* **2004**, *49* (11−12), 41−46.

(8) de Bruin, L. M.; de Kreuk, M. K.; van der Roest, H. F.; Uijterlinde, C.; van Loosdrecht, M. C. M., Aerobic granular sludge technology: an alternative to activated sludge? *Water Sci. Technol.* **2004**, *49* (11−12), 1−7.

(9) Wang, Q.; Du, G. C.; Chen, J. Aerobic granular sludge cultivated under the selective pressure as a driving force. *Process Biochem.* **2004**, *39* (5), 557−563.

(10) Beun, J. J.; Heijnen, J. J.; van Loosdrecht, M. C. M., N-removal in a granular sludge sequencing batch airlift reactor. *Biotechnol. Bioeng.* **2001**, *75* (1), 82−92.

(11) de Kreuk, M. K.; van Loosdrecht, M. C. M. Selection of slow growing organisms as a means for improving aerobic granular sludge stability. *Water Sci. Technol.* **2004**, *49* (11−12), 9−17.

(12) van Loosdrecht, M. C. M.; Hooijmans, C. M.; Brdjanovic, D.; Heijnen, J. J. Biological phosphate removal processes. *Appl. Microbiol. Biotechnol.* **1997**, *48* (3), 289.

(13) de Kreuk, M. K.; Heijnen, J. J.; van Loosdrecht, M. C. M., Simultaneous COD, nitrogen, and phosphate removal by aerobic granular sludge. *Biotechnol. Bioeng.* **2005**, *90* (6), 761−9.

(14) Kreft, J. U.; Booth, G.; Wimpenny, J. W. T., BacSim, a simulator for individual-based modelling of bacterial colony growth. *Microbiol.-SGM* **1998**, *144*, 3275−3287.

(15) Kreft, J. U. Biofilms promote altruism. *Microbiol.-SGM* **2004**, *150*, 2751−2760.

(16) Xavier, J. B.; Foster, K. R. Cooperation and conflict in microbial biofilms. *Proc. Natl. Acad. Sci. U.S.A.* **2007**, *104* (3), 876−81.

(17) Picioreanu, C.; Xavier, J. B.; van Loosdrecht, M. C. M. Advances in mathematical modeling of biofilm structure. *Biofilms* **2005**, *1* (04), 337−349.

(18) Batstone, D. J.; Picioreanu, C.; van Loosdrecht, M. C. Multidimensional modelling to investigate interspecies hydrogen transfer in anaerobic biofilms. *Water Res.* **2006**, *40* (16), 3099−108.

(19) Xavier, J. B.; Picioreanu, C.; van Loosdrecht, M. C. M. A framework for multidimensional modelling of activity and structure of multispecies biofilms. *Environ. Microbiol.* **2005**, *7* (8), 1085−103.

(20) de Kreuk, M. K.; Picioreanu, C.; Hosseini, M.; Xavier, J. B.; van Loosdrecht, M. C. M. Kinetic model of a granular sludge SBR - influences on nutrient removal. *Biotechnol. Bioeng.* **2006**, *97*(4), 801−815.

(21) Mosquera-Corral, A.; de Kreuk, M. K.; Heijnen, J. J.; van Loosdrecht, M. C. M. Effects of oxygen concentration on N-removal in an aerobic granular sludge reactor. *Water Res.* **2005**, *39* (12), 2676–86.

(22) Henze, M.; Gujer, W.; Mino, T.; Matsuo, T.; Wentzel, M. C.; Marais, G. V. R.; van Loosdrecht, M. C. M. Activated sludge model no. 2d, ASM2d. *Water Sci. Technol.* **1999**, *39* (1), 165–182.

(23) Morgenroth, E.; Wilderer, P. A. Controlled biomass removal - The key parameter to achieve enhanced biological phosphorus removal in biofilm systems. *Water Sci. Technol.* **1999**, *39* (7), 33–40.

(24) McSwain, B. S.; Irvine, R. L.; Hausner, M.; Wilderer, P. A. Composition and distribution of extracellular polymeric substances in aerobic flocs and granular sludge. *Appl. Environ. Microbiol.* **2005**, *71* (2), 1051–1057.

(25) Beun, J. J.; van Loosdrecht, M. C. M.; Heijnen, J. J. Aerobic granulation in a sequencing batch airlift reactor. *Water Res.* **2002**, *36* (3), 702–12.

(26) McSwain, B. S.; Irvine, R. L.; Wilderer, P. A. Effect of intermittent feeding on aerobic granule structure. *Water Sci. Technol.* **2004**, *49* (11–12), 19–25.

(27) Tay, J. H.; Pan, S.; Tay, S. T.; Ivanov, V.; Liu, Y. The effect of organic loading rate on the aerobic granulation: the development of shear force theory. *Water Sci. Technol.* **2003**, *47* (11), 235–40.

(28) Tay, J. H.; Liu, Q. S.; Liu, Y. Microscopic observation of aerobic granulation in sequential aerobic sludge blanket reactor. *J. Appl Microbiol* **2001**, *91* (1), 168–75.

(29) Tay, J. H.; Liu, Q. S.; Liu, Y. The effect of upflow air velocity on the structure of aerobic granules cultivated in a sequencing batch reactor. *Water Sci. Technol.* **2004**, *49* (11–12), 35–40.

(30) Liu, Y.; Tay, J. H. The essential role of hydrodynamic shear force in the formation of biofilm and granular sludge. *Water Res.* **2002**, *36* (7), 1653–1665.

(31) Tay, J. H.; Liu, Q. S.; Liu, Y. The effects of shear force on the formation, structure and metabolism of aerobic granules. *Appl. Microbiol. Biotechnol.* **2001**, *57* (1–2), 227–233.

(32) Xavier, J. B.; Picioreanu, C.; van Loosdrecht, M. C. M. A modelling study of the activity and structure of biofilms in biological reactors. *Biofilms* **2005**, *1* (04), 377–391.

(33) Reichert, P. Aquasim—A tool for simulation and data-analysis of aquatic systems. *Water Sci. Technol.* **1994**, *30* (2), 21–30.